Modelling and Analytics of Driving-related Energy Performance of Electric Vehicles

Yuan Rong Dexter Neo, Duong Tran, *Member, IEEE*, Yew Ming Yeap,
and Li Hong Idris Lim, *Senior Member, IEEE*

***Abstract*—Large scale adoption of electric vehicles (EV) has yet to be accelerated due to fundamental challenges such as the availability of charging infrastructure, mileage of the EV, as well as the higher lifetime costs associated with the batteries. In order to address these challenges, this paper introduces a framework to model, analyze and visualize the driving-related energy performance of electric vehicles. Based on a case study of real-world data inputs of throttle, brake and road conditions in Singapore, the proposed framework illustrates several findings in terms of modelling accuracy and driving behaviour identification together with visualization and simulation results in open-source Simulation of Urban Mobility software.**

I. Introduction

The greater adoption of transportation electrification has been encouraged by governments worldwide as part of the solution to tackle the problem of global warming and climate change. Recently in Singapore, along with the island-wide electric Mass Rapid Transit (MRT) system, electric vehicles (EVs) including electric taxis, electric buses etc. have also gathered significant momentum in terms of technological developments, infrastructure upgrades and tax incentives. Examples of such platforms in Singapore include the imminent 1,000-EV fleet of the car-sharing company BlueSG, 800-EV fleet of the electric taxi operator HDT, 200 charging stations of Greenlots, and 1,000 charging points of SP Group by 2022. For a dense urban environment, EVs have the remarkable advantages of no tailpipe emissions and no noise pollution, thus locally ensuring a clean atmosphere. Furthermore, they also pave the way for more automated transport system including autonomous vehicles (AVs) and next-generation vehicle-on-demand services in the near future, which will be crucial for the developed nations with ageing populations.

As an urban motoring solution, modern EVs provide not only clean and quiet but also new responsive driving experience to drivers and passengers with the instant torque from electric motor for acceleration as well as regenerative braking for energy-efficient deceleration. In addition, the compact components of EVs such as electric motors and gear reducers often have different characteristics compared with the mechanical counterparts of internal-combustion engines and gearboxes. Besides, both EVs and the associated charging stations nowadays are always integrated with digital platforms to collect data and perform energy management and fleet management. On the other hand, there are some fundamental challenges inhibiting large scale adoption of EVs, such as the availability of charging infrastructure, range of the EVs and the higher lifetime costs of the EV. It is, therefore, imperative to develop a framework to undertake modelling and analytics of EVs in relation to energy performance and driving experience based on the data available on those digital platforms. For the governments, the framework is necessary in order to evaluate the potential impact of EV adoption at national level in consideration of energy and transport towards sustainability, affordability, comfort and convenience. For EV fleet owners, it will help to further optimise their fleet operations. Lastly, for companies that operate EV charging stations, this framework will also be useful in more advanced scheduling coordination between the EVs and the charging points.

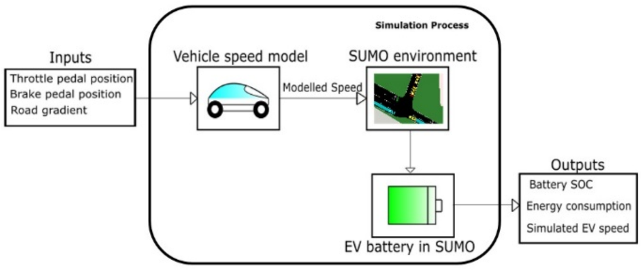

Fig. 1. Overall model of electric vehicles for driving and energy analytics

In literature, there has been research performed on modelling the aerodynamics and energy performance of EVs taking into account several factors such as EV model including electric motor efficiency and torque control, driving behaviour, road conditions etc. By modelling the effect of driving events, energy consumption of EV was identified in conjunction with the behaviours of drivers using inertial sensors in smart phones in [1]. The torque distribution of EV considering efficiency of electric motor was studied in [2]. In Singapore, the energy demand of electric buses for public transport was analysed based on real-world data of large-scale transport networks in [3]. Using big data analysis, the battery for EV was diagnosed for faults and defects in [4]. An EV model was validated against real-world data for the specific Nissan Leaf car using Python-based object-oriented programming approach in [5]. To the best of our understanding, a realistic EV model incorporating real-world data and terrain conditions is not yet available.

In this paper, a framework for modelling EVs based on real-world experimental data is developed, Simulation-based visualisation is examined to investigate the energy performance of the EV and the effects of the driving behaviour on the EV battery as shown in Fig. 1. More specifically, section II provides the details of the vehicle speed model and an equivalent circuit battery model for EV. Section III aims to perform data analytics based on the collected real-world data. Section IV presents the simulation using “Simulation of Urban MObility” (SUMO) followed by the comparative analysis of simulation results with experimental data. Finally, section V concludes the paper.

II. Modelling of Electric Vehicles

For the generalised objectives of an analytical framework, the aerodynamic vehicle model of the EV should be developed. In our work, this model is determined to have three fundamental inputs of throttle pedal position, brake pedal position and road elevation angle. As illustrated in Fig. 1, the output of the vehicle model is the modelled vehicle speed, which in turn is fed into SUMO simulation environment where an identified battery model is used to estimate the state-of-charge (SOC) and the EV energy consumption considering, regenerative braking effect. In addition, this modelled speed and the simulated speed in SUMO can be compared to detect special events during the driving cycles and extract the important features in driving behaviours.

A. *Vehicle longitudinal dynamics model*

For the longitudinal dynamics of EV, Fig. 2 depicts the forces encountered by the vehicle subjected to motion on a slope. The following equations can be derived to describe the longitudinal dynamics of the vehicle [1] [6] [7].

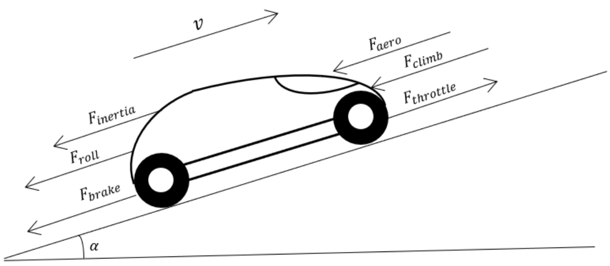

Fig. 2. Longitudinal dynamics model of EV

The aerodynamic drag force of the vehicle F_{aero} is

$$F_{aero} = \frac{1}{2}\rho C_d A v^2 \quad (1)$$

where ρ is the air density, C_d is the coefficient of drag and A is the vehicle frontal area. The grading or climbing force required of the vehicle F_{climb} is

$$F_{climb} = mg\sin\alpha \quad (2)$$

where m is the curb mass of the vehicle, g is the gravitational constant, and α is the angle of elevation of the road. The coefficient of roll f can be calculated using (3), which can be used for a motorcar for speeds up to 128 km/h [8].

$$f = 0.01(1 + \frac{v}{160}) \quad (3)$$

The vehicle rolling resistance F_{roll} is then

$$F_{roll} = mgf\cos\alpha \quad (4)$$

The inertia force encountered by the vehicle $F_{inertia}$ is

$$F_{inertia} = \delta m a \quad (5)$$

where δ is the inertia factor for all rotating components of the vehicle, and a is the acceleration of the vehicle.

By applying Newton's 2nd Law of motion and combining the above equations, we can obtain the differential equation for the motion of the vehicle

$$\frac{dv}{dt} = \frac{1}{m}[F_{throttle} - F_{aero} - F_{roll} - F_{inertia} - F_{brake}] \quad (6)$$

where $F_{throttle}$ and F_{brake} are the two forces controlled by the driver through throttle input and brake input respectively. The throttle input (%) controls the electrical current applied to the drivetrain of the EV, resulting in a change of torque and velocity of the vehicle. The brake input (%) controls both the stopping force and regenerative braking effect of the EV. The throttle and brake inputs are used to derive $F_{throttle}$ and F_{brake} respectively.

B. *Transmission system model*

The tractive effort $F_{tractive}$ of the EV is related to the torque from the electric motor as:

$$F_{tractive} = \frac{T\, G_{ratio}\, \eta_m}{r} \quad (7)$$

where T is torque, G_{ratio} is the transmission ratio, η_m is the motor efficiency, and r is the wheel radius. The mechanical power then can be calculated as

$$P_M = T\omega \quad (8)$$

where ω is angular speed of the motor (rad/s). Assuming electrical power from battery is controlled via pulse width modulation (PWM) from throttle signal, the electrical power required is then

$$P_E = uP_{batt}\eta_e \quad (9)$$

where u is throttle signal, P_{batt} is maximum power from battery, and η_e is energy efficiency of the drivetrain.

C. *Battery model*

For battery modelling, an equivalent circuit model (ECM) is used to describe the battery dynamic behaviours by accurately reproducing the voltage response of the actual battery [9]. The ECM is widely used due to its simplicity and ability to relate the input and output behaviour of the battery cell. Electrical circuit elements, typically in the form of RC network branches are commonly used to represent the ECM [10]. From review of literature, the 2-RC ECM is typically used to represent the battery cell model as an optimal balance between complexity and accuracy. However, the 1-RC ECM is favoured when dealing with battery cells with large inherent hysteresis [11]. Therefore, the 1-RC ECM is chosen for this paper, as shown in Fig. 3. It consists of an ohmic resistor R_0, the parallel 1-RC branch in series and the battery's open circuit voltage (V_{oc}) which is a constant voltage source directly dependent on the battery SOC, internal temperature T_i and the number of charge/discharge cycles N_C [12] [13]. The output battery terminal voltage $V_{terminal}$ is equal to the V_{oc} when the battery terminal current is zero.

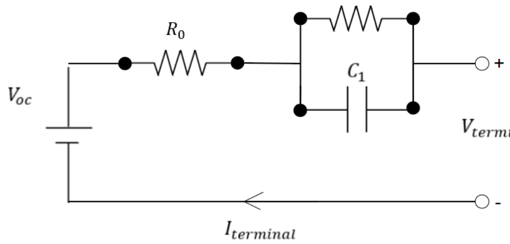

Fig. 3. Equivalent circuit model of EV battery

Neglecting the effect of parasitic elements, open circuit voltage V_{oc} can be described as

$$V_{oc} = f(SOC, T_i, N_C) \tag{10}$$

For the scope of this paper, only the effect of SOC will be considered for the calculation of V_{oc}, the hysteresis effect is also ignored. Therefore, V_{oc} is simplified as

$$V_{oc} = f(SOC) \tag{11}$$

III. Analytics of Real-World Data for Electric Vehicles

In this section, the experimental speed data is filtered to eliminate high-frequency noise. In addition, the Global Positioning System (GPS) trace and altitude data are procured to identify the road gradient required for simulation. Last but not the least, factors such as the wheel radius, gear transmission ratio as well as an estimate of battery model are identified.

A. Data preprocessing

Incoming data from in-vehicle data acquisition modules inherently contain undesirable noise and inaccuracies. As an example, Fig. 4(a) shows the data of throttle pedal and brake pedal being pressed continuously over time of approximately 500s. In the real world, the driver would not be pressing both pedals simultaneously over such a long period of time. Therefore, these inaccuracies in the raw data require to be identified and removed. This can be easily done in the data preprocessing stage by using visualisation and heuristic rules with predefined practical constraints.

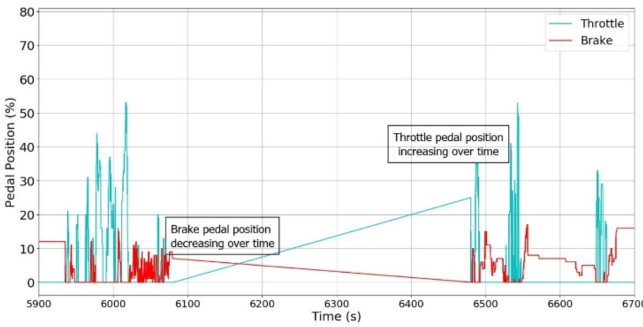

(a) Example of inaccurate/missing data on EV pedals in real world

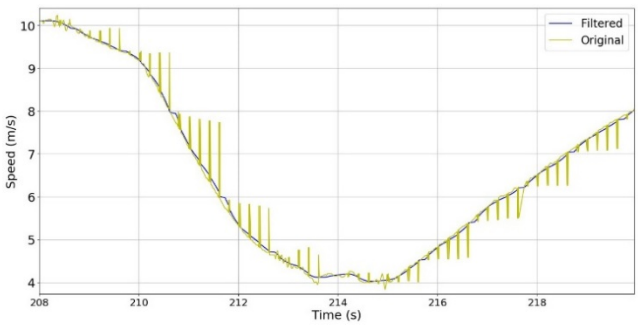

(b) Filtering out noise in vehicle speed data

Fig. 4. Noise and inaccuracy of the real-world data

Apart from accurate reference from the experimental data, it is also necessary to derive other profiles from it. However, the derived results will be unrealistic if the noise is not cancelled out. An example would be to take the derivative of the speed profile in order to obtain the acceleration profile of the EV. To overcome this problem of the noisy data, in data preprocessing stage, a low-pass filter (LPF) can be implemented to filter the unwanted noise from the speed profile, as shown in Fig. 4(b). The filter of choice is an infinite impulse response (IIR) Butterworth filter. The characteristics of the filter and its performance are shown in Table 1.

TABLE 1. PREPROCESSING OF SPEED DATA

Butterworth filter		
Parameter	***Value***	***Unit***
Filter order	6	
Sampling frequency	10	kHz
Cutoff frequency	175	Hz
Performance		
Indicator	***Score***	
R-squared	0.9989	
RMSE	0.1094	

B. Vehicle GPS data and road gradient information

Given the GPS coordinates of the EV, we can visualize the EV trace and obtain the altitude data with the help of the online free utility GPSVisualiser. With the altitude data, the road gradient information can then be obtained and used for (2) and (4) as required in the vehicle longitudinal dynamics model. Based on the GPS trace for one experimental EV route, the road gradient during the drive is derived and illustrated in Fig. 5.

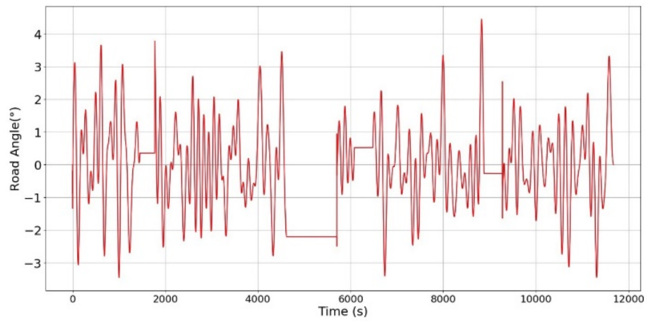

Fig. 5. Altitude profile obtained from GPSVisualiser and the road gradient for the experimental route

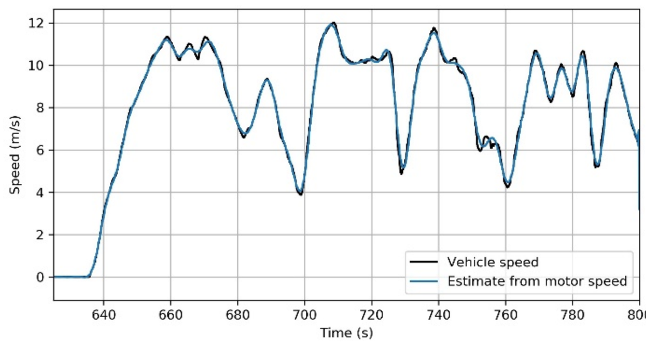

Fig. 6. Correlating vehicle speed and motor speed of EV

C. Vehicle motion

It should be noted that using the well-known vehicle longitudinal dynamics model presented in subsection II.A directly with real-world data will result in remarkable inaccuracies. This is typically due to lack of information of the powertrain and the characteristics of the Electronic Stability Control (ESC) of the vehicle. In practice, manufacturers of EVs do not want to publish this information. Therefore, from the perspective of data analytical framework, it is necessary to apply data analysis techniques to model and extract important features from such a kind of black box. The first step is to identify the characteristics of the gear reducers or virtual gearboxes. This can be obtained by correlating the vehicle speed and the motor speed if available. For this case study, the real-world data indicate high correlation of vehicle speed and motor speed where the factors of wheel radius and constant transmission gear ratio are incorporated, as depicted in Fig. 6. The constants used for the case study are listed in Table 2.

TABLE 2. CONSTANTS ASSUMED FOR ANALYTICS AND SIMULATION

Parameter	Value	Unit
Vehicle frontal area A	3	m^2
Coefficient of drag C_d	0.48	
Inertia factor δ	1.000425	
Gravity of Earth g	9.81	m/s^2
Vehicle curb weight m	2420	kg
Wheel radius r	0.2156	m
Air density ρ	1.196	kg/m^3
Drive-train propulsion efficiency η_e	0.9	
Regenerative braking efficiency η_{regen}	0.55	
Transmission ratio G_{ratio}	3.89	
Motor efficiency η_m	0.90	

After the identification of the characteristics of the EV gear reducers, the next step is to examine the torque profile of the EV as a function of motor speed and throttle position. As illustrated in Fig. 7, in our case study, the torque profile clearly depicts the two main regions of constant torque at low speed, and constant power at medium and high speed.

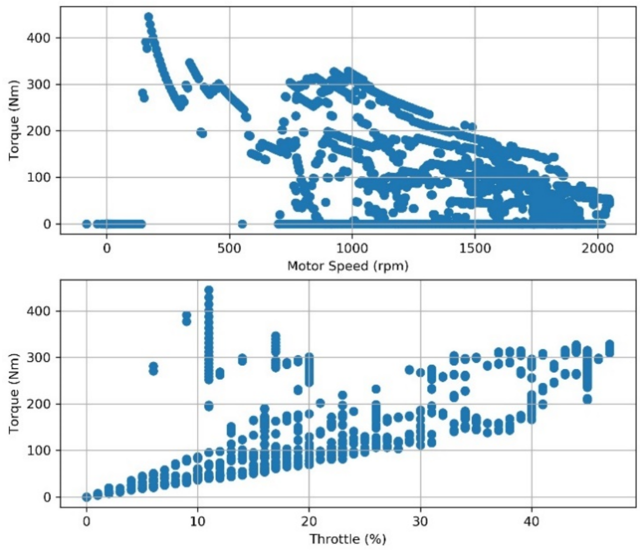

Fig. 7. Torque profile of EV related to motor speed and throttle position

Finally, the last step of feature extraction of the ESC is to adjust the tractive force compensation factors in consideration of the effects of the vehicle speed, the grading force and the rolling resistance force. The results for a driving cycle are shown in Fig. 8 with grading force compensation factor of 0.6 and rolling resistance compensation factor of 3.2. The mean absolute error between actual speed and modelled speed is 0.6190 m/s. As shown, the modelled speed is close to the actual EV speed during periods where change in speed is not significant.

D. Battery

From literature, battery ECM techniques include discrete-time system identification [14] [15], continuous-time system identification [16], electrochemical impedance spectroscopy (EIS) methods [17] [18], and study of the voltage response from current pulse tests [19] [20]. Typically, the open circuit voltage V_{oc} of the battery cell can be measured experimentally at different SOC points with the usage of current pulse tests [21]. This method, however, can require many days. In this paper, an analytical solution is proposed to obtain the estimate of the true V_{oc} and ECM values of R_0, R_1, C_1. The main characteristics for the $LiFePO_4$ battery cell test data in use are listed in Table 3, where the rated capacity of the cell is 2.4Wh.

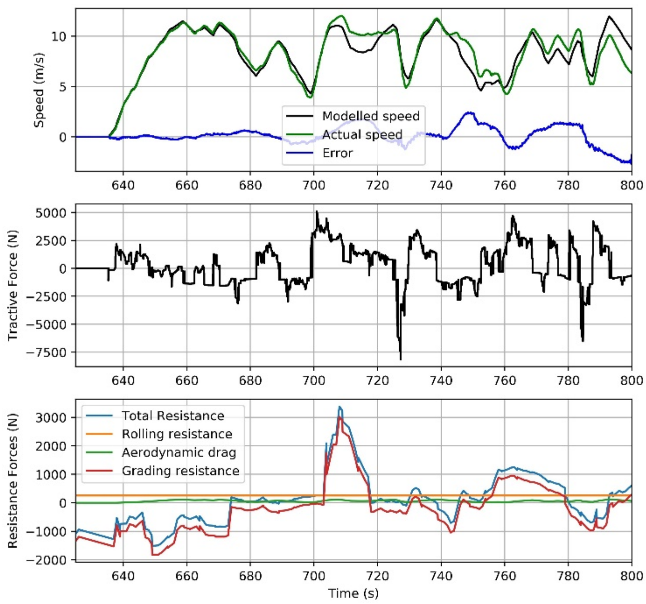

Fig. 8. Comparison of actual EV speed and modelled speed together with tractive force and resistance forces

TABLE 3. EXPERIMENTAL BATTERY CELL CHARACTERISTICS

Mode	Charging phase	Discharging phase
Constant Current (CC)	1.5A until battery voltage reached 4.2V	2A until battery voltage fell to 2.7V
Constant Voltage (CV)	Until charge current dropped to 20mA	

As illustrated in Fig. 9(a), an estimate of R_0, R_1, C_1 can be done by examining the terminal voltage. This yields the initial estimates to be $R_0 = 0.3\Omega$, $R_1 = 0.1285\Omega$, and $C_1 = 13988.33F$. By using (12), the time-response of the current $I_{R_1}(t)$ across resistor R_1 can be obtained as

$$I_{R_1}(t) = I_{terminal} + (I_{R_1}(0) - I_{terminal})e^{-\frac{t}{\tau_1}} \qquad (12)$$

where $\tau_1 = R_1 C_1$ is the time constant, and $I_{terminal}$ is the terminal current. With the initial estimates of the RC parameters, the V_{oc} of the ECM can be obtained by working backwards from the terminal voltage by using (12) – (14).

$$\dot{V}_{\tau_1} = -\frac{V_{\tau_1}}{\tau_1} + \frac{I_{terminal}}{C_1} \tag{13}$$

$$V_{terminal} = Voc \pm V_{\tau_1} \pm R_0 I_{terminal} \tag{14}$$

A brute-force method is used to finetune the RC parameters by substituting them into equations (12)-(14) and using *GridSearchCV*() method in Python-based *scikit-learn* machine learning library. The estimate of true Voc is shown in the $Voc - SOC$ curve of Fig. 9(b), where the final RC parameters are $R_0 = 0.0001\Omega$, $R_1 = 0.1285\Omega$, and $C_1 = 349.7\text{F}$. The curve-fitting toolbox in MATLAB can be employed to obtain the relationship of (11) where the coefficients of the model are found as:

$$V_{OC}(\text{SOC}) = 0.2456\text{SOC}^9 + 0.2381\text{SOC}^8 - 0.8228\text{SOC}^7 - 0.6813\text{SOC}^6 + 0.9252\text{SOC}^5 + 0.5634\text{SOC}^4 - 0.3701\text{SOC}^3 - 0.0582\text{SOC}^2 + 0.2454\text{SOC} + 3.889 \tag{15}$$

with a fitting degree of RMSE of 0.0125, and R-square of 0.9977.

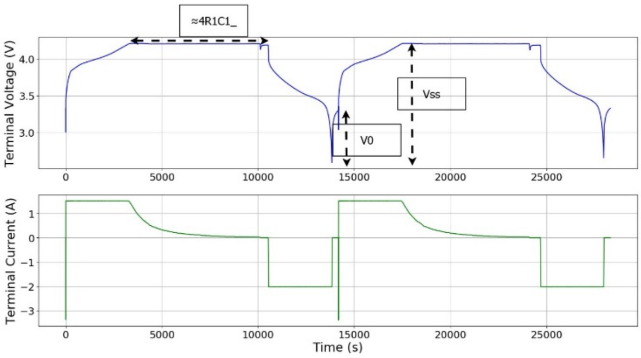

(a) Examining terminal voltage

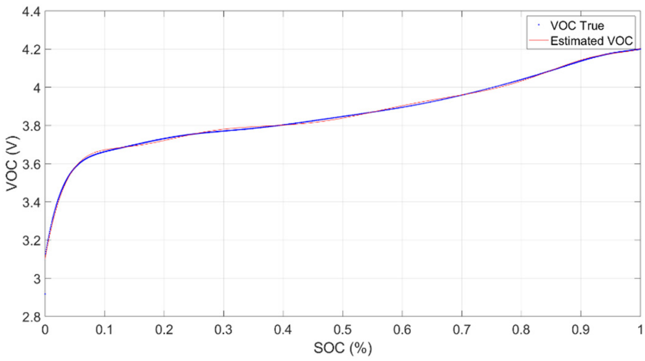

(b) Curve-fitting of open circuit voltage

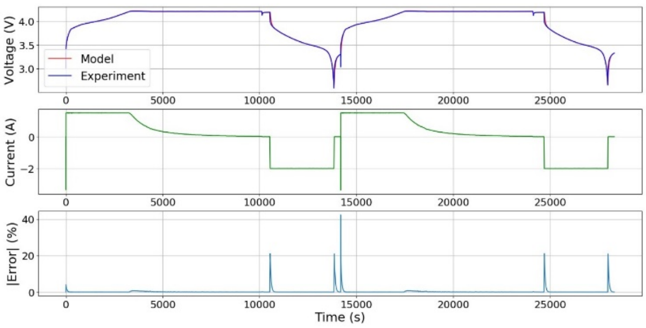

(c) Final result of battery modelling

Fig. 9. Estimate of battery open circuit voltage based on experimental data

IV. Simulation Results and Analysis

The theory-based models described in the previous sections are coded in Python and linked to SUMO by using the Python-Traffic Control Interface (TraCI) protocol.

A. *Defining the road network in SUMO*

The circuit of the experimental EV can be exported from OpenStreetMap (OSM) to SUMO in an XML network file. As Singapore practises left-hand driving, modifications are made to the network file by using the NETCONVERT tool. It is noted that altitude information can also be included in the network file [22]. However, this is not required as the effects of the road gradient have already been considered in the vehicle speed model in section II.

B. *Simulation of the EV*

The parameters of the simulated EV in SUMO can be defined according to the parameters discussed in previous sections, the simulated EV in SUMO has a maximum battery capacity of 80kWh and a maximum power of 90kW. The auxiliary power of the simulated EV is considered as a constant of 857W. The speed of the simulated EV is set based on the modelled speed from the previous section. In [23], realistic driver-centric simulations are developed in the Unity-3D game engine, the driver's steering wheel inputs are considered for the vehicle's trajectory. However, in the scope of this paper, the trajectory of the simulated vehicle will be based on the GPS trace of the experimental EV.

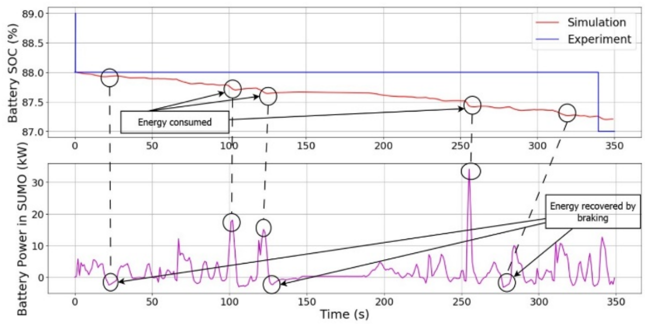

Fig. 10. Comparison of simulated and experimental SOC with profile from SUMO

C. *Simulation results*

By running the above simulation scenario in SUMO, the speed of the simulated EV, battery capacity and energy consumption of the simulated EV can be easily obtained using the TraCI protocol. The energy consumption model in SUMO is based on the change of the simulated vehicle's energy content which can be described by a set of discrete equations [24]. Fig. 11 illustrates the results from the simulation where the experimental EV SOC drops from 88% to 87% and the simulated EV SOC drops from 88% to 87.2%. The simulation in SUMO provides a SOC profile of higher resolution as compared to the experimental EV and is also able to show the energy consumed during the drive or the energy recovered from braking. The matching trend of the battery SOC profiles can be further verified by looking at the energy consumption of the simulated EV and the driver's throttle and brake inputs. Moreover, it is shown that the brake inputs result in negative battery power, due to the electrical current being returned to the battery in the opposite direction with regenerative braking.

It is also observed that there is no additional battery power consumption where the EV is stationary and peak throttle inputs result in peak battery power output.

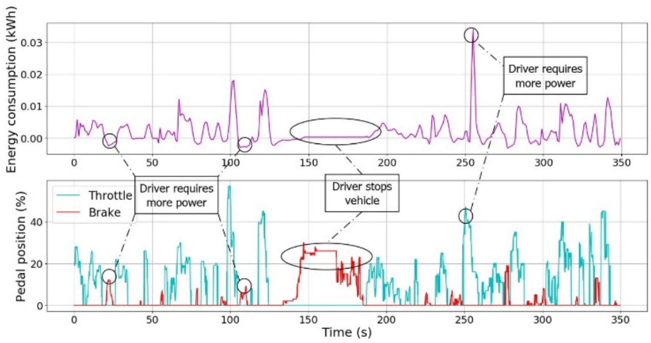

Fig. 11. Illustration of experimental throttle and brake inputs to the simulated energy consumption profile from SUMO

V. CONCLUSION

In this paper, a framework for modelling EVs is presented with accurate vehicle dynamics and battery modelling. The modelling results are then used in the SUMO simulation platform where the relationship between the energy performance and driving behaviours are shown. Several techniques and methods have been effectively utilised to overcome practical problems of noises in real-world data, lack of accurate parameters for modelling, etc. It is shown that the trend of the driving inputs such as throttle and brake pedal position matches those of battery SOC profiles and EV's energy consumption. The framework, therefore, can be further applied to the larger scale of EV fleets to study their impacts on Singapore's road network and charging infrastructures in the future.

REFERENCES

[1] D. Jiménez, H. Sara, J. Fraile-Ardanuy, J. Serrano, R. Fernández and F. Álvarez, "Modelling the effect of driving events on electrical vehicle energy consumption using inertial sensors in smartphones," *Energies,* vol. 11, no. 412, 2018.

[2] J. Park, H. Jeong, I. G. Jang and S.-H. Hwang, "Torque distribution algorithm for an independently driven electric vehicle using a fuzzy control method," *Energies,* vol. 8, pp. 8537 - 8561, 2015.

[3] M. Gallet, T. Massier and T. Hamacher, "Estimation of the energy demand of electric buses based on real-world data for large-scale public transport networks," *Applied Energy,* no. 230, pp. 344 - 356, 2018.

[4] Y. Zhao, P. Liu, Z. Wang, L. Zhang and J. Hong, "Fault and defect diagnosis of battery for electric vehicles based on big data analysis methods," *Applied Energy,* no. 207, pp. 354 -362, 2017.

[5] S. Howroyd and R. Thring, "An electric vehicle model and validation using a Nissan Leaf: A Python-based object-oriented programming approach," *Advances in Mechanical Engineering,* vol. 10, no. 7, pp. 1 - 7, 2018.

[6] "Introduction to Hybrid and Electric Vehicles," NPTEL, 2019. [Online]. Available: https://nptel.ac.in/downloads/108103009/. [Accessed March 2019].

[7] M. P. O'Keefe, A. Simpson, K. J. Kelly and D. S. Pedersen, "Duty cycle characterization and evaluation towards heavy hybrid vehicle applications," doi:10.4271/2007-01-0302, SAE World Congress and Exhibition, Detroit, Michigan, 2007.

[8] M. Ehsani , Y. Gao and A. Emadi, Modern electric, hybrid electric, and fuel cell vehicles: fundamentals, theory, and design, CRC Press; 2 edition, 2009.

[9] M. Kneissl, C. Hametner and M. Dohr, "Nonlinear battery modeling using continuous-time system identification methods and non-uniformly sampled data," in *22nd International Conference on System Theory, Control and Computing (ICSTCC)*, Sinaia, Romania , 2018.

[10] B. Xia, X. Zhao, R. de Callafon, H. Garnier, T. Nguyen and C. Mi, "Accurate Lithium-ion battery parameter estimation with continuous-time system identification methods Accurate Lithium-ion battery parameter estimation with continuous-time system identification methods," *Applied Energy,* vol. 179, pp. 426-436, 2016.

[11] S. Nejad, D. Gladwin and D. Stone, "A systematic review of lumped-parameter equivalent circuit models for real-time estimation of lithium-ion battery states," *Journal of Power Sources,* vol. 316, pp. 183-196, 2016.

[12] R. Zhang, . B. Xia, B. Li, L. Cao, Y. Lai, W. Zheng, H. Wang, W. Wang and M. Wang, "A study on the open circuit voltage and state of charge characterization of high capacity lithium-ion battery under different temperature," *Energies,* vol. 11, no. 2408, 2018.

[13] M. Zhang, Z. Miao and L. Fan, "Battery identification based on real-world data," in *2017 North American Power Symposium (NAPS)*, Morgantown, WV, USA , 17-19 Sept. 2017 .

[14] R. Xiong, F. Sun, H. He and T. D. Nguyen, "A data-driven adaptive state of charge and power capability joint estimator of lithium-ion polymer battery used in electric vehicles," *Energy,* vol. 63, p. 295–308, 2013.

[15] H. Rahimi-Eichi, F. Baronti and M.-Y. Chow, "Modeling and online parameter identification of Li-Polymer battery cells for SOC estimation," in *IEEE International Symposium on Industrial Electronics*, Hangzhou, China, 2012.

[16] B. Xia, X. Zhao, R. de Callafon, H. Garnier, T. Nguyen and C. Mi, "Accurate Lithium-ion battery parameter estimation with continuous-time system identification methods Accurate Lithium-ion battery parameter estimation with continuous-time system identification methods," *Applied Energy,* vol. 179, pp. 426-436, 2016.

[17] P. Vyroubal and T. Kazda, "Equivalent circuit model parameters extraction for lithium ion batteries using electrochemical impedance spectroscopy," *Journal of Energy Storage,* vol. 15, pp. 23-31, 2018.

[18] J. Xu, C. C. Mi, B. Cao and J. Cao, "A new method to estimate the state of charge of lithium-ion batteries based on the battery impedance model," *Journal of Power Sources,* vol. 233, pp. 277-284, 2013.

[19] I. Baccouche, S. Jemmali, B. Manai, N. Omar and N. Essoukri Ben Amara, "Improved OCV model of a Li-Ion NMC battery for online SOC estimation using the extended Kalman filter," *Energies,* vol. 10, no. 764, 2017.

[20] Y. Zou, X. Hu, H. Ma and S. E. Li, "Combined State of Charge and State of Health estimation over lithium-ion battery cell cycle lifespan for electric vehicles," *Journal of Power Sources,* vol. 273, pp. 793-803, 2015.

[21] Y. Diab, F. Auger, E. Schaeffer and M. Wahbeh, "Estimating lithium-ion battery State of Charge and parameters using a continuous-discrete extended Kalman filter," *Energies,* vol. 10, no. 8, p. 1075, 2017.

[22] R. Maia, M. Silva, R. Araújo and U. Nunes, "Electric vehicle simulator for energy consumption studies in electric mobility systems," in *IEEE Forum on Integrated and Sustainable Transportation Systems*, Vienna, Austria , 2011.

[23] C. Olaverri-Monreal, J. Errea-Moreno, A. Díaz-Álvarez , C. Biurrun-Quel, L. Serrano-Arriezu and M. Kuba, "Connection of the SUMO microscopic traffic simulator and the Unity 3D game engine to evaluate V2X communication-based systems," *Sensors (Basel),* 2018.

[24] "Reports of the DLR-Institute of Transportation Systems, Volume 21," The DLR-Institute of Transportation Systems, Berlin-Adlershof, Germany, 2013.